A 298-million-year-old gleicheniaceous fern from China

He, Xuezhi; Zhou, Weiming; Li, Dandan; Wang, Shijun ; Hilton, Jason; Wang, Jun

DOI:
10.1016/j.revpalbo.2020.104355

A 298-million-year-old gleicheniaceous fern from China

Xuezhi He [a,b], Weiming Zhou [b], Dandan Li[b, c], Shijun Wang [d], Jason Hilton [e], Jun Wang [b, c, *]

[a] *Anhui Geological Museum, Hefei 230031, P.R. China*

[b] *State Key Laboratory of Palaeobiology and Stratigraphy (LPS), Nanjing Institute of Geology and Palaeontology and Center for Excellence in Life and Paleoenvironment, Chinese Academy of Sciences, Nanjing 210008, P.R. China*

[c] *University of Chinese Academy of Sciences, No. 19(A) Yuquan Road, Beijing 100049, P.R. China*

[d] *State Key Laboratory of Systematic and Evolutionary Botany (LSB), Institute of Botany, Chinese Academy of Sciences, Beijing 100093, P.R. China*

[e] *School of Geography, Earth and Environmental Sciences, University of Birmingham, Edgbaston, Birmingham B15 2TT, UK*

*Corresponding author.

E-mail address: jun.wang@nigpas.ac.cn (J. Wang)

Highlights

- Early Permian gleicheniaceous rachis with anatomical structure
- Whole-plant reconstruction proposed with rachis, fertile and vegetative fronds

- Earliest stratigraphical occurrence of a member of the Gleicheniaceae documented
- Gleicheniaceae diverged from other ferns by 298.34±0.09 million years ago

ABSTRACT

The late Paleozoic genera *Chansitheca* Regè*, Oligocarpia* Göppert and *Szea* Z. Yao et T. N. Taylor are small ferns that represent putative early members of the Gleicheniaceae based on their morphology and the anatomy of their fertile organs. However, the rachis and cauline anatomy are unknown, rendering their systematic affinities controversial. Here we document rachides with partly preserved anatomical structure associated with compression/impression specimens of *Chansitheca wudaensis* from the Wuda Tuff Flora. The *in situ* preservation of the flora, occasional organic connection and close association, and matching size, proportions and xylem structure indicate that these rachides belonged to the same plant that produced fertile fronds of the *Chansitheca wudaensis* type and vegetative fronds of the *Sphenopteris* type co-occurring in this flora. The new details of the anatomy and morphology necessitate emendations to the diagnosis for this species. As the Wuda Tuff Flora has been dated to be 298.34±0.09 million years ago (Asselian, Permian), this represents the oldest unequivocal evidence of Gleicheniaceae. Our results thus demonstrate that the Gleicheniaceae had already diverged from other ferns families, including the Osmundaceae, by this time.

Key word: Gleicheniaceae, *Chansitheca wudaensis*, rachial anatomy, Permian, Asselian

1. Introduction

Extant members of the Gleicheniaceae are mainly found in tropical and subtropical regions in both the Old and New World, and encompass about 120–150 species belonging to six genera that include *Dicranopteris* Bernhardi, *Gleichenia* Smith, *Sticherus* Presl, *Diplopterygium* (Diels) Nakai, *Gleichenella* Ching, and *Stromatopteris* Mettenius (Bower, 1926; Kramer, 1990; Mickel and Smith, 2004; Perrie et al., 2007). They are characterized by rhizomes with "vitalized" protosteles or rarely solenosteles, pseudo-dichotomously forked fronds caused by a resting bud (except for the monotypic genus *Stromatopteris*), exindusiate sori with simultaneous maturation and large, round sporangia with a transverse-oblique annulus (Bower, 1926; Smith et al., 2006). Phylogenetic relationships of the Gleicheniaceae from cladistic analyses of morphological and molecular data (e.g., Pryer et al., 2004; Pryer et al., 2001; Pryer et al., 1995; Schneider et al., 2004; Schuettpelz et al., 2006; Smith et al., 2006; Wikström and Pryer, 2005; Wolf, 1997; Wolf et al., 1998) demonstrate they are monophyletic and closely related to the Dipteridaceae and Matoniaceae (Smith et al., 2006).

In the fossil record, gleicheniaceous ferns are rare in the Paleozoic but become more abundant during the Mesozoic. Fertile and vegetative fronds bearing lobed and pecopteroid foliage have been ascribed to the genera *Gleichenia* and *Gleichenites* Göppert. However, Nagalingum and Cantrill (2006), among others, pointed out that the genus *Gleichenites* is invalid as the original specimens have been reassigned as members of the seed ferns. Nevertheless, the genus name *Gleichenites* continues to be

widely used to refer to both fossil foliage and spores (e.g., Taylor et al., 2009). Gleicheniaceous fossil plants with preserved cauline and rachis anatomical structure are known from Cretaceous and younger strata, including *Gleichenia chaloneri* Herendeen et Skog (Herendeen and Skog, 1998), *Boodlepteris turoniana* Gandolfo et al. (Gandolfo et al., 1997) and *Gleichenia appianensis* Mindell et al. (Mindell et al., 2006). However, even such materials were not readily linked to any extant lineage (Perrie et al., 2007).

From the Paleozoic, *Oligocarpia* Göppert, *Szea* Z. Yao et T.N. Taylor, *Chansitheca* Regè and *Henanotheca* Yang are all considered to be members of the Gleicheniales (e.g., Abbott, 1954; He et al., 2016; Regè, 1920; Stevens and Hilton, 2009; Taylor et al., 2009; Wang et al., 1999b; Wang and Wu, 1999; Yang, 2006; Yao and Taylor, 1988). *Oligocarpia*, a reproductive organ from the Carboniferous, has been treated as the earliest member of the family (Abbott, 1954; Taylor et al., 2009), while the oldest unambiguous evidence for such affiliation based on spore-wall ultrastructure is from the Permian, *O. kepingensis* Y.D. Wang et X.Y. Wu (Wang and Wu, 1999). However, *Oligocarpia* has also been regarded as belonging to the Sermayaceae (Eggert and Delevoryas, 1967; Taylor et al., 2009), based on finds of reproductive organs of *Oligocarpia* in organic attachment to an *Anachoropteris*-type rachis (Eggert and Delevoryas, 1967). *Szea*, *Henanotheca* and *Chansitheca* are reproductive organs that all show characters in general agreement with those of gleicheniaceous ferns, but the rachides and stems of the plants that borne these reproductive organs are still unknown. Although numerous species were established

for Paleozoic rachides and stems with anatomical preservation, none show the entire suite of characters indicating affinities with the Gleicheniaceae (Taylor et al., 2009).

From 2007 to 2018, tens of thousands of fossil plant specimens were excavated from the Wuda Tuff Flora (Wang et al., 2013), the so-called "vegetational Pompeii" (Wang et al., 2012). This instantaneously preserved early Permian flora (Bashforth and DiMichele, 2012; Wang et al., 2012) occurs in the 66 cm thick volcanic tuff between the No. 7 and No. 6 coal seams in the Wuda Coalfield (Pfefferkorn and Wang, 2007; Wang et al., 2012; Wang et al., 2013). Amongst the large fossil assemblage recovered, only a few dozens of specimens of *Chansitheca wudaensis* Deng et al. (Deng et al., 2000) were discovered. These reproductive organs containing *in situ* spores have been described in detail (Deng et al., 2000; He et al., 2016), but the petiolar and cauline anatomy of the plant that produced them remained unknown. In the present study, antepenultimate rachides, and rachides associated with fertile and vegetative foliage of *C. wudaensis* are described from the Wuda Tuff Flora and a review of *C. wudaensis* is given. We here present evidence that the associated rachides belong to the *C. wudaensis* plant.

2. Geological information

The Ordos Basin contains abundant petroleum and coal resources and is a secondary tectonic unit on the west of the North China Plate. During most of the Permian, it formed a separate, large island in the tropics between the Tethys and Panthallassic oceans (Wang et al., 1990; Ziegler et al., 1997; Guo and Liu, 2000). The

basin is constrained by the Yingshan and Daqing Mountains in the north, the Long and Qiaoshan Mountain in the south, the Helan and Liupanshan Mountain in the west, and the Lvliang-Taihang Mountain in the east (Wang, 1996). The basin itself is a tectonic basin formed by the superposition and transformation of multi-stage coal-accumulating basins, with coal-accumulation controlled by the conversion process of Caledonian-Hercynian tectonic movements (Wang, 2011). The Wuda Coalfield occurs at the northwestern margin of the Ordos Basin, northwestern of Wuhai City, Inner Mongolia Autonomous Region of North China (Fig. 1).

The Permian lithological units exposed in and around the Wuda Coalfield from the bottom to the top consist of the Taiyuan, Shanxi and Lower Shihhotse formations (Wan et al., 2016; Liang et al., 2019). During the Permian, deltaic sedimentary environments dominated this region (Wang et al., 2002); sedimentary microfacies analysis indicates that the coal seams intercalated in the Taiyuan Formation were deposited in deltaic plain sedimentary environments (Wang et al., 2016).

Palaeobiogeographically, the Wuda Coalfield belongs to the North China phytogeographical realm (Shen, 1995; Shen et al., 1996; Wang and Shen, 1996; Wang et al., 1999a). The Cisuralian (early Permian) plants of this area are generally quite similar to those of central North China (Halle, 1927; Lee, 1963; He et al., 1995; Wang, 2010). During recent decades, fossil plant assemblages from the Taiyuan and Shanxi formations have been subjected to detailed investigations. Taxonomy, anatomy, sedimentology and taphonomy was combined to reveal the environment changes and the forest succession, especially the assemblages from the No. 7 and No. 6 coal seams

of the Taiyuan Formation (e.g., Pfefferkorn and Wang, 2007; Wang et al., 2012; Zhou et al., 2015; Liang et al., 2019). Four successive floras were recognized in the c. 5 m thick section from the underclay of the No. 7 coal seam to the roof-shale of the No. 6 coal seam (Fig. 1; Pfefferkorn and Wang, 2007). Identification and quantitative analyses of the Wuda Tuff Flora allowed the reconstruction of more than 1000 m^2 of peat-forming forest (Wang et al., 2012). Seven groups of the plants compose the peat-forming vegetation, including Lycopsida, Sphenopsida, pteridophytes, Noeggerathiales, pteridosperms (seed ferns), Cycadopsida and cordaitalean coniferophytes.

The Wuda Tuff comprises predominantly kaolinite clay and quartz crystals. U-Pb dating from zircon crystals in the tuff have determined a radiometric age of 298.34±0.09 Ma (Schmitz et al., 2020; this issue), thus placing the tuff in the Asselian Stage of the Permian. The Rare Earth Element (REE) distribution of the tuff is characterized by the enrichment of light rare earth elements (LREE) and negative δEu values that indicates the tuff derived from a felsic volcano, and the magma derived from a magmatic arc (Wang M. et al., 2020).

3. Materials and methods

Most of the specimens of *Chansitheca wudaensis* were collected from the lower part of the Wuda Tuff horizon. In the collections, 68 *Chansitheca wudaensis* specimens were examined and four specimens show the anatomical structure of the rachides.

111 Anatomically preserved rachides were cut into pieces for making transverse and
112 longitudinal sections. All sections were prepared by the acetate peel technique (Galtier
113 and Phillips, 1999). Individual surfaces were successively ground on a glass plate
114 using #600 and #1000 carborundum grift, and etched using HF (concentration ＜10%)
115 for 120 seconds. Peels were mounted on glass slides using neutral balsam and a cover
116 slip.
117 Macrofossils were immersed in pure ethyl alcohol and photographed using a
118 Nikon D800 digital camera with a 60 mm macro lens (Kerp and Bomfleur, 2011).
119 Detail of the rachis and sorus were photographed using a Carl Zeiss STEMI 2000-C
120 stereomicroscope and DLC300-L digital camera using “dlc performance” software.
121 Microphotographs of slides were photographed using a Carl Zeiss Axio Scope A1
122 polar transmitted microscope with a digital camera ProgRes C5 using ProgRes
123 CapturePro 2.8 software. Multi-focus-level stacking was used and photomosaics were
124 composed by stitching together composite large photographs from smaller individual
125 images.
126
127 **4. Systematic palaeobotany**
128 *Family:* Gleicheniaceae (R. Brown 1810) C. Presl 1825
129 *Genus:* ***Chansitheca*** Regè 1920.
130 *Species:* ***Chansitheca wudaensis*** Deng, Sun et Li emended He et al. (Plates I–VI,
131 Fig. 2)
132 *Repository:* All preparations are from the same specimens, deposited in the

Palaeobotany collections of the Nanjing Institute of Geology and Palaeontology, Chinese Academy of Sciences, with registration numbers PB 23071, PB 23278, PB23279 and PB 23280.

Locality: Wuda Coalfield in Wuhai City, Inner Mongolia Autonomous Region, North China.

Geological horizon: Lower part of the tuff between the Coal 7 and Coal 6, the upper most part of the Taiyuan Formation.

Stratigraphic age: Asselian (early Permian), 298.34±0.09 Ma.

Emended diagnosis: Frond at least bipinnate. Various order rachides and pinnule midribs slightly flexuose. Penultimate rachides slender, with fine longitudinal striation. Penultimate pinnae lanceolate, with contracted base, lobed in basal and middle portions; in anadromous parts less strongly lobed, with 4–6 pairs of lobes. Midrib slightly decurrent, forming a 60–70° angle to the ultimate rachis. Lateral veins sympodial-dichotomously branched in lobes in the basal and middle portions of the pinnules, and less branched in lobes in the upper part of a pinnule. Sori abaxial, attached to the ends of lateral veins, without indusium, 2–4 per lobe. Sorus ovate to elliptical, length/width ratio c. 1.5, with 4–10 sporangia, commonly 6–7. Sporangia sessile, annulate, 200–400 μm in diameter, sub-triangular, pyriform or rectangular. Annulus transversal, encircling middle to basal part, formed by 17–22 pairs of elongated thick-walled cells, occasionally three cells high. Stomium composed of narrow and elongate cells extending to basal part of sporangium. Spores trilete, 21.05–26.31 μm in diameter, exine smooth, with round to subtriangular amb;

interradial area straight or convex, radial areas rounded. Laesurae straight and concave, extending to 2/3–3/4 of spore radius. Narrow interradial thickenings present along and parallel to laesurae. Rachis with xylem adaxially recurved, C-shaped, 2–6 (mostly 2–4) cells thick, with or without strongly furled ends; 4–15 protoxylem poles distributed along recurved face of the xylem. Metaxylem tracheids near furled ends and xylem ends much smaller than in other places. Metaxylem tracheid walls possessing uni- to multiseriate scalariform thickenings. Phloem adjacent to internal face of xylem, absent from external face. Prickles, as small spines, and ridges developed on upper side of rachis.

Remarks: The diagnosis presented above represents the characterization of the whole-plant based on information recovered from a single bed in the Wuda coalfield. The reconstruction is based on specimens in organic attachment and intricate associations of morphologically similar specimens.

Description: Four specimens are demonstrated here to show the relationship between the rachides and fertile fronds of *Chansitheca wudaensis*. Two of them show the antepenultimate rachis of *C. wudaensis* (Plate I, 1–4), while the other two represent rachides that are preserved intricately associated with *C. wudaensis* (Plate I, 5–8). The antepenultimate and associated rachides are about 7 mm thick (Plate I). The transverse sections of the specimens shown in Plate I, 1, 2 and 5 were made from the position marked by the dashed line. To obtain transverse sections of the rachis of the specimen in Plate I, 6, the original slab was cut into five parts marked A–E, with the cutting planes numbered 1 through 8 (Figure 2). A longitudinal section was made

177 from part E. After making the transverse sections, the surface of part C (Figure 2;
178 Plate I, 7, 8) was prepared and showed that the fertile fronds are not in organic
179 connection with the rachis.

180 The xylem strands in the transverse sections of antepenultimate rachides are
181 well-preserved and form an arc or an open C-shape (Plate II, 1–6; Figure 3 A). Four
182 protoxylem strands are present at the internal face of the xylem strand and the
183 metaxylem normally consists of 2–4 layers of tracheids (Plate II, 2–6). Tracheids of
184 the metaxylem are polygonal with smaller-sized tracheids (18–39 μm) at the internal
185 side and larger tracheids (45–72 μm) in the middle and at the external side of the
186 vascular bundle (Plate II, 1–6). At the end of the xylem strand, the tracheid size is
187 reduced to 7–22 μm × 10–20 μm. On the epidermis, ridges are developed on the
188 adaxial side of the rachis (Plate II, 1–2, 4–6) and consist of elongated polygonal
189 parenchyma cells (Plate II, 6). The phloem and the cortex are not preserved.

190 The anatomical structure of the associated rachis of specimen PB 23280 is
191 imperfectly preserved (Plate II, 7, 8). However, the anatomical structure of the rachis
192 of specimen PB 23071 is preserved much better (Plate III). Although the associated
193 rachides are preserved differently, the xylem and phloem structures are quite similar.
194 The end of xylem strand is strongly enrolled with the protoxylem strand attached at
195 the internal face (Plate II, 7, 8). The phloem is present at the internal side of the xylem
196 strand (Plate II, 7, 8). Internal to the xylem, the phloem is differentiated into an outer
197 parenchymatous layer and an inner sclerotic, fibrous layer of thick-walled cells close
198 to the xylem (Plate II, 7).

The rachis structure of specimen PB 23071 is better preserved and less affected by compaction. The outline of the rachis is asymmetrical and the xylem eccentric in oblique and transverse sections of the rachis of specimen PB 23071 (Plate I, 6; Plate III, 1, 2; Figure 2). The epidermis is represented by a structureless 10–40 μm thick dark layer surrounding the rachis (Plate III, 1, 2). Epidermal hairs are present to the right side (Plate III, 1). Ridges and prickles in the form of small spines are also developed on the upper side of the rachis (Plate III, 2). In transverse section, the rachis is c. 6 mm wide and c. 2.5 mm thick (Plate III, 2). The end of the C-shaped xylem is 2–4 tracheids thick with strongly enrolled ends (Plate III, 2, 3; Figure 3 B). Some parts of the xylem are separated by dark cells of the phloem (Plate III, 1; Plate III, 2, 3).

Tracheids of the metaxylem are polygonal and with smaller tracheids (10–35 μm) at the internal side and larger tracheids (50–100 μm) in the middle part and external side of the vascular bundle (Plate III, 3). The xylem at the junction of the arch and enrolled arms is constricted, and tracheid size is reduced to 6–26 × 14–34 μm (Plate III, 1). On the transverse/tangential sections, most of the tracheids in the xylem strand are isodiametric or slightly tangentially elongate (Plate III, 3 rectangle frame). Individual tracheids are elongate and 54–91 μm (typically 60–80 μm) long and 35–90 μm wide, or isodiametric in diameter. Some very small and round tracheid clusters occur at the internal side of the xylem (Plate III, 3 arrows; Plate IV, 1, 2). These small tracheid clusters are interpreted as protoxylem poles of which fifteen are recognized (Plate III, 3 arrows). In some protoxylem strands, individual tracheids are crushed

(Plate IV, 4) but where they are intact, they are generally in round in section (Plate IV, 2). Protoxylem tracheids are surrounded by large tracheids, showing endarch maturation (Plate IV, 1, 2).

The phloem on the internal side of the xylem is well-preserved, whereas most of the phloem on the external side is not preserved (Plate III, 1–3). Internal to the xylem, the phloem is differentiated into an outer parenchymatous layer that is 20–120 μm thick and comprised of cells with irregular shapes and sizes (Plate III, 3; Plate IV, 2, 3), and an inner sclerotic, fibrous layer of thick-walled cells close to the xylem (Plate III, 1, 3; Plate IV, 1–4). Intercellular spaces are schizogenous and well-developed (Plate IV, 4). The long axes of the cells in the phloem are along the tangential direction (Plate IV, 3).

Most of the cortex is not preserved (Plate III, 1, 2), except for some parenchyma cells adjacent to the epidermis (Plate IV, 5, 6). These cells are irregular in shape, c. 30–40 μm long and 15–25 μm wide, with sinuous cell walls. The long axis of the cells is oriented along the tangential direction (Plate IV, 5, 6). Because this tissue is mostly absent, we consider that it was entirely parenchymatous.

Surface ornamentation on the rachis includes ridges, prickles (small spines) and unidentified appendages (Plate III, 1, 2). The ridges are strongly coalified to a degree that structural details are indistinguishable (Plate III, 2). The prickles are triangular at the base with long needle-like tips (Plate III, 2). The basal part of the unidentified appendages is composed of irregular parenchyma cells (Plate V, 1). The cells in the prickles and adjacent tissues are small, typically from 15 to 40 μm. Wall

243 protuberances occur at the internal cell walls (Plate V, 2).

244 Longitudinal sections through the rachis were all made from Part E. The lowest
245 section shows the ornamentation on the adaxial rachis surface (Plate V, 3–5). Two
246 clusters of cells are present on the adaxial rachis surface (Plate V, 3). The cells in the
247 smaller elliptical cluster are quadrangular and pentagonal, c. 50 μm in diameter and
248 approximately half of them are filled with dark material (Plate V, 4). The cells in the
249 larger lanceolate cluster are elongated polygons, considerably varying in size from 20
250 to 150 μm (Plate V, 5). When the longitudinal section cuts through the C-shaped
251 xylem and the strongly enrolled ends, the distribution of protoxylem (Plate V, 6 white
252 arrows), metaxylem and phloem can be easily observed (Plate V, 6; Plate VI, 3). Some
253 protoxylem tracheids with annular thickenings were destroyed (Plate VI, 1). In some
254 protoxylem tracheids, there are obvious spiral thickenings (Plate VI, 2, 5). Metaxylem
255 tracheids have scalariform thickenings. On narrow metaxylem tracheids, the
256 scalariform thickenings are uniseriate, while it is multiseriate in wider ones. Septa are
257 present in some wide metaxylem tracheids (Plate VI, 3 arrow). The phloem is dark- to
258 light-brown and the parenchyma cells are almost rectangular (Plate VI, 6). Because of
259 imperfect preservation, pits have not been observed (Plate VI, 6).

260

261 **5. Discussion**

262 5.1. Characterizing the *Chansitheca wudaensis* plant.

263 The associated rachis described here belongs to the fertile frond of *Chansitheca*
264 *wudaensis* in the Wuda Tuff Flora. The flora represents an instantaneously preserved

in situ fossil assemblage with minimal transport, and lacks post-depositional disturbance such as burrowing or reworking. This indicates the close affinity of the rachis to *C. wudaensis* in the source flora prior to the ash fall event. More important is that the width of the associated rachides always matches that of antepenultimate rachis of *C. wudaensis* fertile fronds. The rachides preserved associated with the fertile fronds have the same anatomical structure. Furthermore, the xylem structure, tracheids and ornamentation of the associated rachides are nearly identical to those of the antepenultimate rachides of *C. wudaensis*. There are some differences between the xylem of the antepenultimate and associated rachides, for instance, the strongly enrolled ends of the xylem and the large number of protoxylem strands, which are not observed in antepenultimate rachides. Furthermore, phloem is absent in antepenultimate rachides. Such differences may be caused by different preservation situation and/or different ontogenic stages for the antepenultimate and the associated rachides. Such differences are to be expected in different organs of the same plant species.

Chansitheca wudaensis is known from the morphology of the fertile frond comprising naked sori, abaxially attached to the ends of the lateral veins, 2–4 in each lobe; the sorus is ovate to elliptic, with 4–10 sessile annulate sporangia. The annulus is transverse, encircling the middle to basal part of the sporangia. Spores are trilete, 21–26 μm in diameter, and have a smooth exine. Laesurae are straight and concave, extending to 2/3 – 3/4 of the spore radius (He et al., 2016). These features are exclusively present in extant and fossil members of the Gleicheniaceae (e.g., Boodle,

1901; Ogura, 1972; Smith et al., 2006) from which we infer an affinity or close relationship of this fossil to the Gleicheniaceae. However, its cauline anatomy is still unknown. The anatomical structure and size of the associated rachides and antepenultimate rachides of *C. wudaensis* are very similar and lend strong support that they are from a single whole-plant species (see Bateman and Hilton, 2009), as does their intricate association in the tuff. We consider that the associated rachides and fertile fronds belong to the same whole-plant species. As in previous studies (He et al., 2016), we conclude that the vegetative fronds of *C. wudaensis* were of the *Sphenopteris*-type, which are also frequent in the Wuda tuff horizon, although there not found in close association with the rachides. The frond is at least bipinnate. The penultimate and ultimate pinnae are lanceolate. Lobed pinnules are lanceolate, with a contracted base. Lateral veins are sympodial-dichotomously branched in the lobes. We propose that these fossil plant species constituted a single whole-plant species sensu Bateman and Hilton (2009) that represents the earliest stratigraphic representative of the Gleicheniaceae.

5.2. Comparison and affinity on the rachis structure

During the late Paleozoic, several fern groups were characterized by C-shaped petiolar xylem strands. Among these, the petiolar xylem of the Anachoropteridaceae, Kaplanopteridaceae, Psalixochlaenaceae and Sermayaceae is abaxially curved, whereas that of Psaroniaceae and Osmundales is adaxially curved (Ogura, 1972; Taylor et al., 2009; Galtier and Phillips, 2014; Wang et al., 2014b). The rachis

described here is similar to that of marattialean fern *Psaronius* and members of the Osmundales in having adaxially curved xylem and also in its position of their protoxylem strands. However, the rachis in *Psaronius* can be distinguished from the species described here in the features of its tracheid thickenings. Tracheids in the rachis of members of the Psaroniaceae have uniseriate scalariform thickening (He et al., 2013; Wang S.-J. et al., 2020, in this issue), whereas in *Chansitheca wudaensis* the rachis it is uni- to multiseriate. Within the Osmundales, the rachis structure is very similar to that of *C. wudaensis* and it is difficult to distinguish them based on their xylem. However, in *C. wudaensis*, the rachis has xylem tracheids that are constricted at the junction of the arch (Wang et al., 2014a). Vegetative and fertile fronds belonging to members of the Osmundales are absent in the Wuda Tuff Flora, whereas the here described rachides occur in intricate association with fertile fronds of the putative gleicheniaceous fern *C. wudaensis* of which vegetative anatomy was so far unknown.

Anatomically preserved rhizomes or petioles of Gleicheniaceae are rare in the fossil record and most of these records are from the Mesozoic and the Eocene. *Antarctipteris sclericaulis* Millay et Taylor 1990, a rhizome from the Triassic of Antarctica, is assigned to the Gleicheniaceae on the basis of its mixed protostele, simple frond trace, and scalariform tracheids. Unlike the rachis described here, the petiolar xylem of the Antarctic specimens is C- to V-shaped vascular strands giving off primary pinnae with V- to W-shaped vascular traces (Millay and Taylor, 1990), which clearly distinguishes the taxa.

Gleichenia chaloneri Herendeen et Skog 1998, described from fusainized frond segments from the Lower Cretaceous of England, is suggested as sister species to the extant species *Gleichenia glauca*, based on cladistic analysis (Herendeen and Skog, 1998). *Gleichenia chaloneri* rachides resemble *Chansitheca wudaensis* rachides in their simple C-shaped xylem; numerous protoxylem strands are present on the adaxial side of the bundle and the features of its scalariform tracheid thickenings, although the range of the number of protoxylem strands is larger in the latter. In the rachis of *G. chaloneri*, tracheids are often in a single row unlike those in the *C. wudaensis* rachides.

Boodlepteris turoniana Gandolfo et al. 1997, described from charcoalified remains from the Turonian (Late Cretaceous) of New Jersey, has been interpreted as a sister species to the extant genus *Stromatopteris*. The petiole of *B. turoniana* is similar to the rachides from Wuda in having a C-shaped vascular bundle, endarch primary-xylem maturation and scalariform thickened tracheids. However, there are many more protoxylem strands in the rachis from Wuda than in *B. turoniana*. The size of the rachis is another difference between *B. turoniana* and the Wuda rachis, with the petiole of *B. turoniana* being 0.8–1.4 mm in diameter (Gandolfo et al., 1997), while the rachis from Wuda is much larger and is 6 × 2.5 mm in diameter.

Gleichenia appianensis Mindell et al. 2006 was described from a permineralized rhizome and associated vegetative remains from the Eocene of British Columbia. *G. appianensis* frond segments share several characters with the rachis of *Chansitheca wudaensis*, including an inwardly folded and adaxially curved, C-shaped xylem,

353 numerous (five or more) protoxylem strands showing endarch maturation, scalariform
354 tracheids and regularly spaced horizontal septations. Mindell et al. (2006) mentioned
355 that the septa in the metaxylem tracheids of the frond trace is a feature unknown in the
356 extant *Gleichenia*, but such septa probably represent tyloses, which have been
357 observed in the stipes of numerous fern families (Ogura, 1972) and specifically in the
358 protoxylem of *Gleichenia* (Chrysler, 1943). In the rachis of *G. appianensis*, tracheids
359 are constricted at the lateral edges of the trace, whereas in the *C. wudaensis* rachis, the
360 tracheids are constricted at the inwardly folded arms.
361
362 5.3. Ornamentation
363 In extant gleicheniaceous ferns, ornamentation is commonly present on the
364 resting bud and on the abaxial side of the juvenile frond rachis (Boodle, 1901; Ogura,
365 1972; Lu, 2007), but the function is insufficiently known. Small prickles are
366 non-vascularized outgrowth from the surface of plant organs (Simpson, 2010). The
367 sharp-pointed tips usually provide physical defense against animals such as herbivores.
368 In some of the modern plant groups such as Rosaceae, prickles as hooked structures
369 could also produce frictional resistance for the function of scrambling (Gallenmüller
370 et al., 2015). In the late Paleozoic fossil record they sometimes were regarded as an
371 indicator of the vine- or liana-like growth habit (e.g., Li and Taylor, 1998; Krings et
372 al., 2001). However, *Chansitheca wudaensis* fronds with prickles on the rachis surface
373 are not associated with large tree trunks on which they could have climbed. During
374 field excavations, fronds of *C. wudaensis* were mainly preserved in the lower part of

375 the tuff bed and are in this context unlikely to have dropped from the treetops prior to
376 burial. On the other hand, the fronds of *C. wudaensis* were found preserved in clusters
377 and with individual specimens overlapping other (Plate I). This indicates *C.*
378 *wudaensis* may have grown in clumps or thickets and the fronds may have lent on on
379 each other providing mutual support like some Carboniferous species of *Medullosa*
380 (Krings et al., 2003). The prickles on the adaxial side forming prickly surfaces may
381 optimize such a growth habit. Furthermore, eight types of insect mediated damage
382 have been discovered on eleven host plant species from the Wuda flora (Feng et al.,
383 2020, in this issue). Although no feeding traces were detected on the *Sphenopteris*
384 fronds that represent the vegetative fronds of the *C. wudaensis* plant (He et al., 2016),
385 comparing with the trichomes on the leaves of *Anomozamites villosus* Pott et al. 2012,
386 the size and density of prickles on rachis of *C. wudaensis* was unlikely to have been
387 effective in warding off herbivorous insects. Therefore, the prickles of the rachis of *C.*
388 *wudaensis* are probably used for optimizing growth in thickets rather than for
389 scrambling or defending against herbivorous insects.
390
391 5.4. Timing the divergence of Gleicheniaceae
392 Previous molecular dating estimates conclude that the earliest divergence of the
393 Gleichenoids (Gleicheniaceae, Dipteridaceae, and Matoniaceae) occurred during the
394 Capitanian Stage of the Permian at approximately 263 Ma (Pryer et al., 2004), with
395 later divergence occurring in the mid-Triassic at approximately 227 Ma (Pryer et al.,
396 2004) coincident with the Carnian-Norian Stage boundary. However, divergences

within each of these families were estimated to be during the Cretaceous (Pryer et al., 2004). Schuettpelz and Pryer (2009) predicted an older divergence for the Gleicheniales at 276 Ma during the Kungurian stage of the Permian, but Pryer et al. (2004) concluded they started to diversify before the end of the Palaeozoic during the Capitanian Stage approximately 14 Ma after their origin. We interpret that the Wuda species of Gleicheniaceae shows an earlier divergence for the Gleichenaceae at 298.34±0.09 Ma, approximately 35 Ma before the earliest divergence time predicted by Pryer et al. (2004) and 20 Ma before that predicted by Schuettpelz and Pryer (2009). We also conclude that the range of other species assigned to the Gleicheniaceae from the Permian (e.g., *Szea sinensis* Yao et Taylor, *Szea henanensis* Yang, Sheng et Wang, *Oligocarpia kerpingensis*) indicates that shortly after their origin, diversification was already underway within the group. The Cretaceous diversification within the family indicated by Pryer et al. (2004) appears to represent a second radiation event within the family.

5.5. Taphonomic consideration in plant morphologic restoration

Plant remains buried in sediments will experience compaction in diagenesis to varying extents and will be compressed and deformed (e.g., Zodrow et al., 2005). This phenomenon has been observed on the petrified sori and the vertically preserved stems in the Wuda Tuff (He et al., 2016; Wang et al., 2013). Transverse sections of gleicheniaceous fern rachides are almost circular, whereas the transverse section of the rachis described here is an asymmetric, lenticular shape (Plate III) that has been

compressed. If we assume that the rachis did not expand laterally during compaction, and the rachis originally is circular with its diameter matching its 6 mm width, the compaction rate of the rachis can be calculated at 0.58 that is slightly larger than the 0.56 calculated for vertically preserved stems in the Wuda Tuff Flora (Wang et al., 2013). The asymmetric rachis and eccentric xylem indicate the existence of slight lateral expansion during compaction (Plate II, 1, 4; Plate III, 1–3). Therefore the compaction rate from the rachis should be slightly smaller than 0.58. The xylem is also affected by the compaction, and the elongated cells on both lateral corners may be caused by compaction, because the directions of the tracheidal short axes consist with the compression direction. The inrolled ends of the C-shaped xylem were nearly crushed (Plate III, 1–2). Therefore, the shape of the xylem may originally have been more circular.

Acknowledgements

We thank Wei Ran (State Key Laboratory of Systematic and Evolutionary Botany (LSB), Institute of Botany, Chinese Academy of Sciences) for help obtaining literature. We thank Mei Shengwu and Cheng Youdong (Nanjing Institute of Geology and Palaeontology, Chinese Academy of Sciences, Nanjing) for help in collecting specimens and experiments. This study was funded jointly by the National Natural Sciences Foundation of China (41702024, 41802011 and 41530101), the Strategic Priority Research Program (B) of Chinese Academy of Sciences (No. XDB18000000 and XDB26000000), the State Key Laboratory of Palaeobiology and Stratigraphy

(Nanjing Institute of Geology and Palaeontology, CAS)(No. 173109 and 20182114), Anhui Geological Museum Collecting, Preparation and Research Fund.

References

Abbott, M.L., 1954. Revision of the Paleozoic fern genus *Oligocarpia*. Palaeontographica Abt. B 96, 39–65.

Bashforth, A.R., DiMichele, W.A., 2012. Permian coal forest offers a glimpse of late Paleozoic ecology. Proc. Nat. Acad. Sci. USA 109, 4717–4718.

Bateman, R.M., Hilton, J., 2009. Palaeobotanical systematics for the phylogenetic age: applying organspecies, form-species and phylogenetic species concepts in a framework of reconstructed fossil and extant whole-plants. Taxon 58, 1254–1280.

Boodle, L.A., 1901. Comparative anatomy of the Hymenophyllaceae, Schizaeaceae and Gleicheniaceae. III. On the anatomy of the Gleicheniaceae. Ann. Bot. XV, 703–747.

Bower, F.O., 1926. The ferns (Filicales). The eusporangiatae and other relatively primitive ferns, vol. II. Cambridge University Press, Cambridge.

Chrysler, M.A., 1943. The vascular structure of *Gleichenia*. I. The anatomy of the branching regions. Amer. J. Bot. 30, 735–743.

Deng, S.-H., Sun, K.-Q., Li, C.-S., 2000. A new Gleicheniaceous fern *Chansitheca* (*Sphenopteris*) *wudaensis* from the lower Permian of Wuda, Nei Mongol, China. Acta Bot. Sin. 42, 533–538.

Eggert, D.A., Delevoryas, T., 1967. Studies of Paleozoic ferns: *Sermaya*, gen. nov.

464 and its bearing on filicalean evolution in the Paleozoic. Palaeontographica Abt. B
465 120, 169–180.
466 Feng, Z., Wang, J., Zhou, W.-M., Wan, M.-L., Pšenička, J., 2020. Plant-insect
467 interactions in the early Permian vegetational Pompeii, Wuda, Northwest China.
468 Rev. Palaeobot. Palynol. (This issue).
469 Gallenmüller, F., Feus, A., Fiedler, K., Speck, T., 2015. Rose prickles and asparagus
470 spines – different hook structures as attachment devices in climbing plants.
471 PLOS ONE 10, e0143850.
472 Galtier, J., Phillips, T.L., 1999. The acetate peel technique. In: Jones, T.P., Rowe, N.P.
473 (Eds.), Fossil Plants and Spores: modern Techniques. Geological Society of
474 London, London, pp. 67–71.
475 Galtier, J., Phillips, T.L., 2014. Evolutionary and ecological perspectives of Late
476 Paleozoic ferns. Part III. Anachoropterid ferns (including *Anachoropteris*,
477 *Tubicaulis*, the Sermayaceae, Kaplanopteridaceae and Psalixochlaenaceae). Rev.
478 Palaeobot. Palynol. 205, 31–73.
479 Gandolfo, M.A., Nixon, K.C., Crepet, W.L., Ratcliffe, G.E., 1997. A new fossil fern
480 assignable to Gleicheniaceae from Late Cretaceous sediments of New Jersey.
481 Amer. J. Bot. 84, 483–493.
482 Guo, Y.-H., Liu, H.-J., 2000. The Late Palaeozoic depositional systems of Shaanxi–
483 Gansu–Ningxia Area. J. Palaeogeog. 2, 19–30.
484 Halle, T.G., 1927. Palaeozoic plants from central Shansi. Palaeontologia Sinica, Ser. A
485 2, 1–316.

He, X.-L., Zhu, M.-L., Fan, B.-H., Zhuang, S.-Q., Ding, H., Xue, Y., 1995. The Late Palaeozoic Stratigraphic Classification, Correlation, and Biota from Eastern Hill of Taiyuan City, Shanxi Province. Jilin University Press, Changchun. (In Chinese, English summary)

He, X.-Y., Wang, S.-J., Hilton, J., Galtier, J., Li, Y.-J., Shao, L.-Y., 2013. A unique trunk of Psaroniaceae (Marattiales)—*Psaronius xuii* sp. nov., and subdivision of the genus *Psaronius* Cotta. Rev. Palaeobot. Palynol. 197, 1–14.

He, X.-Z., Wang, S.-J., Wang, J., 2016. *Chansitheca wudaensis* (Gleicheniaceae, fern) from the early Permian Wuda Tuff Flora, Inner Monglia. Palaeoworld 25, 199–211.

Herendeen, P.S., Skog, J.E., 1998. *Gleichenia chaloneri*—a new fossil fern from the lower Cretaceous (Albian) of England. Int. J. Plant Sci. 159, 870–879.

Kerp, H., Bomfleur, B., 2011. Photography of plant fossils—New techniques, old tricks. Rev. Palaeobot. Palynol. 166, 117–151.

Kramer, K.U., 1990. Gleicheniaceae. In: Kubitzki, K. (Ed.), The families and genera of vascular plants, Volume I. Springer-Verlag, Berlin, pp. 145–152.

Krings, M., Taylor, T.N., Taylor, E.L., Axsmith, B.J., Kerp, H., 2001. Cuticles of *Mariopteris occidentalis* White nov. emend. from the Middle Pennsylvanian of Oklahoma (USA), and a new type of climber hook for mariopteroid pteridosperms. Rev. Palaeobot. Palynol. 114, 209–222.

Krings, M., Kerp, H., Taylor, T.N., Taylor, E.L., 2003. How Paleozoic vines and lianas got off the ground: on scrambling and climbing Carboniferous–Early Permian

508 Pteridosperms. Bot. Rev. 69(2), 204–224.
509 Lee, H.-H., 1963. Fossil plants of the Yuehmenkou Series, North China. Palaeontol.
510 Sin. 6, 1–185 (New series A, Whole Number 148, in Chinese and English).
511 Li, H.-Q., Taylor, D.W., 1998. *Aculeovinea yunguiensis* gen. et sp. nov.
512 (Gigantopteridales), a new taxon of Gigantopterid stem from the Upper Permian
513 of Guizhou Province, China. Int. J. Plant Sci. 159, 1023–1033.
514 Liang, R.-J., Wan, M.-L., Yang, W., Wang, J., 2019. Floor flora of Coal 4 and 5 from
515 the lower Permian Shanxi Formation in Wuda Coalfield, Inner Mongolia. Acta
516 Palaeontol. Sinica 58, 23–46.
517 Lu, S.-G., 2007. Pteridology. Higher Education Press, Beijing.
518 Mickel, J.T., Smith, A.R., 2004. The Pteridophytes of Mexico. Mem. New York Bot.
519 Gard. 88, 1–1054.
520 Millay, M.A., Taylor, T.N., 1990. New fern stems from the Triassic of Antarctica. Rev.
521 Palaeobot. Palynol. 62, 41–64.
522 Mindell, R.A., Stockey, R.A., Rothwell, G.W., Beard, G., 2006. *Gelichenia*
523 *appianensis* sp. nov. (Gleicheniaceae): a permineralized rhizome and associated
524 vegetative remains from the Eocene of Vancouver Island, British Columbia. Int. J.
525 Plant Sci. 167, 639–647.
526 Nagalingum, N.S., Cantrill, D.J., 2006. Early Cretaceous Gleicheniaceae and
527 Matoniaceae (Gleicheniales) from Alexander Island, Antarctica. Rev. Palaeobot.
528 Palynol. 138, 73–93.
529 Ogura, Y., 1972. Comparative anatomy of vegetative organs of the pteridophytes.

530 Gebrüder Borntraeger: Berlin Stuttgart.
531 Perrie, L.R., Bayly, M.J., Lehnebach, C.A., Patrick, B.J., 2007. Molecular
532 phylogenetics and molecular dating of the New Zealand Gleicheniaceae.
533 Brittonia 59, 129–141.
534 Pfefferkorn, H.W., Wang, J., 2007. Early Permian coal-forming floras preserved as
535 compressions from the Wuda District (Inner Mongolia, China). Int. J. Coal Geol.
536 69, 90–102.
537 Pott, C., McLoughlin, S., Wu, S.Q., Friis, E.M., 2012. Trichomes on the leaves of
538 *Anomozamites villosus* sp. nov. (Bennettitales) from the Daohugou beds (Middle
539 Jurassic), Inner Mongolia, China: Mechanical defence against herbivorous
540 arthropods. Rev. Palaeobot. Palynol. 169, 48–60.
541 Pryer, K.M., Schuettpelz, E., Wolf, P.G., Schneider, H., Smith, A.R., Cranfill, R., 2004.
542 Phylogeny and evolution of ferns (Monilophytes) with a focus on the early
543 leptosporangiate divergences. Amer. J. Bot. 91, 1582–1598.
544 Pryer, K.M., Smith, A.R., Hunt, J.S., Dubuisson, J.Y., 2001. *rbc*L data reveal two
545 monophyletic group of filmy ferns (Filicopsida : Hymenophyllaceae). Amer. J.
546 Bot. 88, 1118–1130.
547 Pryer, K.M., Smith, A.R., Skog, J.E., 1995. Phylogenetic relationships of extant ferns
548 based on evidence from morphology and *rbc*L sequences. Amer. J. Bot. 85, 205–
549 282.
550 Regè, R., 1920. Note su alcuni vegetali del Carbonifero della Cina. Atti Società
551 Italiani di Scienze Naturali di Milano 59, 183–197.

552 Schneider, H.E., Smith, A.R., Cranfill, R., Hildebrand, T.E., Haufler, C.H., Ranker,
553 T.A., 2004. Unraveling the phylogeny of polygrammoid ferns (Polypodiaceae
554 and Grammitidaceae): exploring aspects of the diversification of epiphytic plants.
555 Mol. Phy. Evol. 31, 1041–1063.
556 Schmitz, M.D., Pfefferkorn, H.W., Shen, S.Z., Wang, J., 2020. A volcanic tuff near the
557 Carboniferous-Permian boundary, Taiyuan Formation, North China: Radiometric
558 dating and global correlation. Rev. Palaeobot. Palynol. (This issue).
559 Schuettpelz, E., Korall, P., Pryer, K.M., 2006. Plastid *atpA* data provide improved
560 support for deep relationships among ferns. Taxon 55, 897–906.
561 Schuettpelz, E., Pryer, K.M., 2009. Evidence for a Cenozoic radiation of ferns in an
562 angiosperm-dominated canopy. Proc. Natl. Acad. Sci. USA 106, 11200–11205.
563 Shen, G.-L., 1995. Permian floras. In: Li, X.-X. (Ed.), Fossil Floras of China through
564 the Geological Ages (English Edition). Guangdong Science and Technology
565 Press, Guangzhou, pp. 127–223.
566 Shen, G.-L., Wang, Y.-D., Wang, J., Liu, H.-Q., Zhang, S.-Q., 1996. Tectonic
567 implications of Permian floras in China. Palaeobotanist 45, 324–328.
568 Simpson, M.G., 2010. Plant systematics, Second ed. Burlington: Academic Pres.
569 Smith, A.R., Pryer, K.M., Schuettpelz, E., Korall, P., Schneider, H., Wolf, P.G., 2006.
570 A classification for extant ferns. Taxon 55, 705–731.
571 Stevens, L.G., Hilton, J., 2009. Ontogeny and ecology of the Filicalean fern
572 *Oligocarpia gothanii* (Gleicheniaceae) from the Middle Permian of China. Amer.
573 J. Bot. 96, 475–486.

574 Taylor, T.N., Taylor, E.L., Krings, M., 2009. Paleobotany: the biology and evolution
575 of fossil plants, 2nd edition. Academic Press, Boston.
576 Wan, M.-L., Zhou, W.-M., He, X.-Z., Liu, L.-J., Wang, J., 2016. A typical
577 Euramerican floral element from the Shanxi Formation (Cisuralian, lower
578 Permian) in the Wuda Coal Field, Inner Mongolia, North China. Palaeobiod.
579 Palaeoenviron. 96, 507-515.
580 Wang, H.-Z., Yang, S.-P., Zhu, H., Zhang, L.-H., Li, X., 1990. Palaeozoic
581 biogeography of China and adjacent regions and world reconstruction of the
582 palaeocontinents. In: Wang, H.Z., Yang, S.P., Liu, B.P., et al., (Eds.),
583 Tectonopalaeogeography and Palaeobiogeography of China and Adjacent
584 Regions. China University Geosciences Press, Beijing, pp. 35–38.
585 Wang, J., 2010. Late Paleozoic macrofloral assemblages from Weibei Coalfield, with
586 reference to vegetational change through the Late Paleozoic Ice-age in the North
587 China Block. Int. J. Coal Geol. 83, 292–317.
588 Wang, J., He, X.-Z., Pfefferkorn, H.W., Wang, J.-R., 2013. Compaction rate of an
589 early Permian volcanic tuff from Wuda Coalfield, Inner Mongolia. Acta Geol.
590 Sinica (English Edition) 87, 1242–1249.
591 Wang, J., Pfefferkorn, H.W., Zhang, Y., Feng, Z., 2012. Permian vegetational Pompeii
592 from Inner Mongolia and its implications for landscape paleoecology and
593 paleobiogeography of Cathaysia. Proc. Natl. Acad. Sci. USA 109, 4927–4932.
594 Wang, J., Shen, G.-L., 1996. Permian phytogeography of China. Palaeobotanist 45,
595 272–277.

596 Wang, J., Zhang, Q.-X., Shen, G.-L., 1999a. Permian phytogeography of Cathaysian
597 flora in China in the light of cluster analysis. Acta Palaeontol. Sin. 38, 530–543.
598 Wang, M., Zhong, Y.-T, He, B., Denyszyn, S.W., Wang, J., Xu, Y.-G, 2020.
599 Geochronology and geochemistry of the fossil-flora-bearing Wuda Tuff in North
600 China Craton and its tectonic implications. Lithos 2020.
601 doi:10.1016/j.lithos.2020.105485.
602 Wang, S.-J., Hilton, J., Galtier, J., He, X.-Y., Shao, L.-Y., 2014a. *Tiania yunnanense*
603 gen. et sp. nov., an osmundalean stem from the Upper Permian of southwestern
604 China previously placed within *Palaeosmunda*. Rev. Palaeobot. Palynol. 210,
605 37–49.
606 Wang, S.-J., Hilton, J., He, X.-Y., Seyfullah, L.J., Shao, L.-Y, 2014b. The
607 anatomically preserved stem *Zhongmingella* gen. nov. from the Upper Permian
608 of China: evaluating the early evolution and phylogeny of the Osmundales. J.
609 Syst. Palaeontol. 12, 1–22.
610 Wang, S.-J., Wang, J., Liu, L.-J., Hilton, J., 2020. Stem diversity in the marattialean
611 tree fern family Psaroniaceae from the earliest Permian Wuda Tuff Flora. Rev.
612 Palaeobot. Palynol. (This issue)
613 Wang, S.-M., 1996. Coal accumulation and coal resource evaluation of Ordos Basin.
614 China Coal Industry Publishing House, Beijing.
615 Wang, S.-M., 2011. Ordos Basin tectonic evolution and structural control of coal.
616 Geol. Bull. China 30, 544–552.
617 Wang, W.-H., Tian, J.-C., Wang, F., 2016. Research on sedimentary environment and

618 distribution of coal seam of Taiyuan Formation in Erdos Basin. Coal Tech. 35,
619 125–126.
620 Wang, Y.-D., Guignard, G., Barale, G., 1999b. Morphological and ultrastructural
621 studies on *in situ* spores of *Oligocarpia* (Gleicheniaceae) from the lower Permian
622 of Xinjiang, China. Int. J. Plant Sci. 160, 1035–1045.
623 Wang, Y.-D, Wu, X.-Y., 1999. *Oligocarpia kepingensis* sp. nov. from the Lower
624 Permian of the northern Tarim Basin, Xinjiang and itsin situ spores. Chinese Sci.
625 Bull. 44, 108–112.
626 Wang, Z.-J., Chen, H.-D., Zhang, J.-Q., 2002. The Late Palaeozoic sedimentary
627 systems and humic gas pools in the Ordos Basin. Sedimentary Geology Tethyan
628 Geology 22, 18–23.
629 Wikström, N., Pryer, K.M., 2005. Incongruence between primary sequence data and
630 the distribution of a mitochondrial atp1 group II intron among ferns and
631 horsetails. Mol. Phylog. Evol. 36, 484–493.
632 Wolf, P.G., 1997. Evaluation of atpB nucleotide sequences for phylogenetic studies of
633 ferns and other pteridophytes. Amer. J. Bot. 84, 1429–1440.
634 Wolf, P.G., Pryer, K.M., Smith, A.R., Hasebe, M., 1998. Phylogenetic studies of
635 extant pteridophytes. In: Soltis, E.D., Soltis, S.P., Doyle, J.J. (Eds.), Molecular
636 systematics of plant, vol. 2, DNA sequencing. Kluwer Academis Publishers,
637 Boston, USA, 541–556.
638 Yang, G.-X., 2006. The Permian Cathaysian Flora in western Henan Province, China.
639 Geological Publishing House, Beijing.

Yao, Z.-Q., Taylor, T.N., 1988. On a new gleicheniaceous fern from the Permian of south China. Rev. Palaeobot. Palynol. 54, 121–134.

Zhou, W.-M., Wan, M.-L., Yan, M.-X., Cheng, C., Wang, J., 2015. The succession sequence of early Permian wetland vegetational communities in the Shanxi Formation of the Wuda Coalfield, Inner Mongolia. Acta Palaeontol. Sinica 54, 66–83.

Ziegler, A.M., Hulver, M.L., Rowley, D.B., 1997. Permian world topography and climate. In: Martini, I.P. (Ed.), Late glacial and postglacial environmental change, Quaternary, Carboniferous–Permian, and Proterozoic. Oxford University Press, Oxford and New York, pp. 111–146.

Zodrow, E.L., Pšenička, J., Bek, J., 2005. A reassessment of the taxonomy of *Oligocarpia bellii* (Late Pennsylvanian, Sydney Coalfield, Nova Scotia, Canada). Palaeotographica Abt. B 272, 51-65.

Figure and Plate Captions

Figure 1. Locality maps and outcrop sections of the tuff bed in the Wuda Coalfield. A. Outline map showing position of the Ordos Basin; B. Map of the Ordos Basin showing main geological units and structural features (modified after Li, 2009); C. Summary geological map of the Wuda Coalfield; D, E. Outcrop and lithological column of the No. 7 and 6 Coal Seams and the tuff bed in between. The oldest flora (Flora 1) was rooted in the underclay and initiated peat accumulation that led to the formation of the lower coal (Coal 7), which is overlain by the volcanic tuff. In the middle-lower part of the tuff bed, a second flora (Flora 2, the Wuda Tuff Flora) is

663 preserved, which grew on the peat at the time of the ash-fall. The upper part of the tuff
664 was rooted by a single lycopsid species (Flora 3), again initiating peat accumulation
665 (Coal 6). The roof-shale of Coal 6 yielded the fourth flora, representing the vegetation
666 that lived around a lake that flooded the coal swamp.
667
668 Figure 2. Location of saw cuts for preparation of specimen PB 23071, preparing five
669 parts numbered A–E, with cut surfaces numbered 1–8. Scale bar = 1 cm
670
671 Figure 3. Schematic diagram showing the structure of the antepenultimate rachis of
672 *Chansitheca wudaensis* and associated rachis. px: protoxylem; ph: phloem; r: ridge; x:
673 xylem. A. antepenultimate rachis of *Chansitheca wudaensis*; B. associated rachis.
674
675 Plate I. *Chansitheca wudaensis* fertile fronds showing antepenult rachides and
676 associated rachides; dashes indicate cutting positions.
677 1, 2. *Chansitheca wudaensis* fertile fronds showing antepenultimate rachis. Scale bar
678 = 2 cm. Specimen in 1 is PB 23278 and 2 is PB 23279.
679 3. Detail of Plate I, 2, showing the organic connection between the antepenultimate
680 and penultimate rachis. Scale bar = 2 mm.
681 4. Detail of Plate I, 2, showing an ultimate pinna and sori. Scale bar = 2 mm.
682 5. The thick rachis associated with fertile fronds of *Chansitheca wudaensis*. Specimen
683 PB 23280. Scale bar = 1 cm.
684 6. The rachis (arrow) preserved with *Chansitheca wudaensis* fertile fronds that are at

different depth in the matrix. Specimen PB 23071. Scale bar = 1 cm.

7. Part C of figure 2 with complete surface preparation of specimen PB 23071, showing the relationship of *Chansitheca wudaensis* fertile frond (white arrows) and associated rachis (black arrow). Scale bar = 1 cm.

8. Detail of Plate I, 7 showing the ultimate pinna and pinnules with sori. Scale bar = 1mm

Plate II. Transverse sections from antepenultimate rachides of *Chansitheca wudaensis* and associated rachis. ep = epidermis; px = protoxylem; ph = phloem; r = ridge; x = xylem.

1–3. Transverse sections (slide PB 23278 - T1) from specimen in Plate I, 1 (PB 23278), showing strongly compressed rachis preserved epidermis (ep), xylem and ridge (r). Scale bar = 1000 μm. 2. Detail of Plate II, 1, showing the tracheids and protoxylem (px), the epidermis was compressed and adjacent to the xylem strand. Scale bar= 200 μm. 3. Detail of Plate II, 1, showing the curved end of the xylem strand, arrow indicates protoxylem (px). Scale bar = 200 μm.

4–6. Transverse sections from the specimen PB 23279 (Plate I, 2) showing compressed rachis of *Chansitheca wudaensis* with open C-shaped xylem (x) and 2 ridges (r) at the adaxial side. 4 from slide PB 23279-T1, scale bar = 500 μm. 5 from slide PB 23279-T2, scale bar = 1000 μm. 6. Enlargement from 5, showing detail of the xylem (x), protoxylem (px; arrows) and ridge (r). Scale bar = 200 μm. 7–8. Transverse section of slide PB 23280-T1 from specimen PB 23280 from Plate I, 5.

7. showing C-shaped xylem (x) with furled ends and phloem (ph). Scale bar = 500 μm.

8. Detail of Plate II, 7, showing the xylem (x) and protoxylem (px) (arrow) born at the adaxial side. Scale bar = 1000 μm.

Plate III. Transverse sections (slightly oblique) of the associated rachis from specimen PB 23071 shown in Plate I, 6.

1. Section from cutting surface 1, showing C-shaped vascular bundle with strongly furled ends and ornamentations attached on the epidermis. Slide number AT 1009. Scale bar = 1000 μm.

2, 3. Section from cutting surface 6 with small cortex (c) adjacent epidermis (ep) preserved; ornamentation including ridges (r) and spines (s) present on the epidermis (ep); xylem (x) is C-shaped, and phloem (ph) present at the internal face of the xylem. Slide DT 6010. Scale bar = 1000 μm. 2 Entire transverse section of the rachis, and 3 showing the xylem with multiple protoxylem (px) strands present at the internal side of the C-shaped xylem (arrows).

Plate IV. Details of the xylem and cortex of the associated rachis from specimen PB 23071 shown in Plate I, 6 and Figure 2. Part D cutting surface 6; 1–5 from slide DT 6010; 6 from slide DT 6006.

1, 2. Detail of Plate III, 3, showing the xylem. 1. Protoxylem (px) present at the internal side of the metaxylem (mx), and most cells of the protoxylem were not

729 preserved. Scale bar = 100 μm; 2. Protoxylem and metaxylem on the end of the xylem.
730 Scale bar = 50 μm.
731 3. Detail of Plate III, 3, showing the metaxylem (mx), phloem (ph) and thick-walled
732 fibre cells between them. Scale bar = 100 μm.
733 4. Detail of Plate III, 3, showing the phloem and the well-developed intercellular
734 space (arrow). Scale bar = 20 μm.
735 5, 6. Detail of the cortex adjacent to the epidermis. Scale bar in 5 = 200 μm and in 6 =
736 50 μm.
737
738 Plate V. Details of the ornamentation and the longitudinal sections of the associated
739 rachis of specimen PB 23071 shown in Plate I, 6. 1, 2 are from Part D cutting surface
740 6, slide number DT 6010; 3–6 are from Part E, with 3–5 from slide E 001; 6 is from
741 slide E 006.
742 1, 2. Detail of Plate III, 2. 1 showing the base of a hair. Scale bar = 50 μm. 2. Details
743 of the prickles (small spines) and adjacent tissue. Scale bar = 20 μm.
744 3. Ridges and other ornamentation on the adaxial side of the rachis. Arrow indicates
745 the ridge. Scale bar = 1000 μm.
746 4. Detail of a in Plate V, 3, showing the elliptic base of ornamentation, composed of
747 isodiametric parenchyma cells filled with black material. Scale bar = 200 μm.
748 5. Detail of b in Plate V, 3, showing the lanceolate ornamentation, composed of
749 elongated parenchyma cells. Scale bar = 200 μm.
750 6. Longitudinal section of the xylem, showing the positions of protoxylem (px),

751 metaxylem (mx), phloem (ph) and the epidermis (ep), arrow indicates the protoxylem.
752 Scale bar = 1000 μm.
753
754 Plate VI. Longitudinal sections and details of associated rachis specimen PB 23071
755 shown in Plate I, 6. 1–3 are enlarged from Plate V, 6 from Part E, slide number E006;
756 4–6 are from Part E, slide number E 008.
757 1. Enlargement from frame a in Plate V, 6, showing imperfectly preserved protoxylem
758 (px) and metaxylem (mx) with multiseriate scalariform thickenings. Phloem (ph) is
759 dark. Scale bar = 25 μm.
760 2. Enlargement from frame b in Plate V, 6, showing spiral thickenings on the
761 protoxylem (px) tracheid walls and uniseriate or multiseriate scalariform thickenings
762 on metaxylem (mx) tracheid walls. The adjacent phloem is in dark-colored. Scale bar
763 = 100 μm.
764 3. Septa (arrow) in the multiseriate scalariform thickening tracheids. Scale bar = 25
765 μm.
766 4. Longitudinal section of the rachis showing the entire section. Scale bar = 1000 μm.
767 5. Enlargement from frame a in Plate VI, 4, showing dark brown phloem (ph), spiral
768 thickenings on protoxylem (px) tracheid walls and the scalariform thickenings on
769 metaxylem (mx) tracheid walls. Scale bar = 100 μm.
770 6. Enlargement from frame b in Plate VI, 4, showing the brown phloem (ph). Scale
771 bar = 100 μm.
772

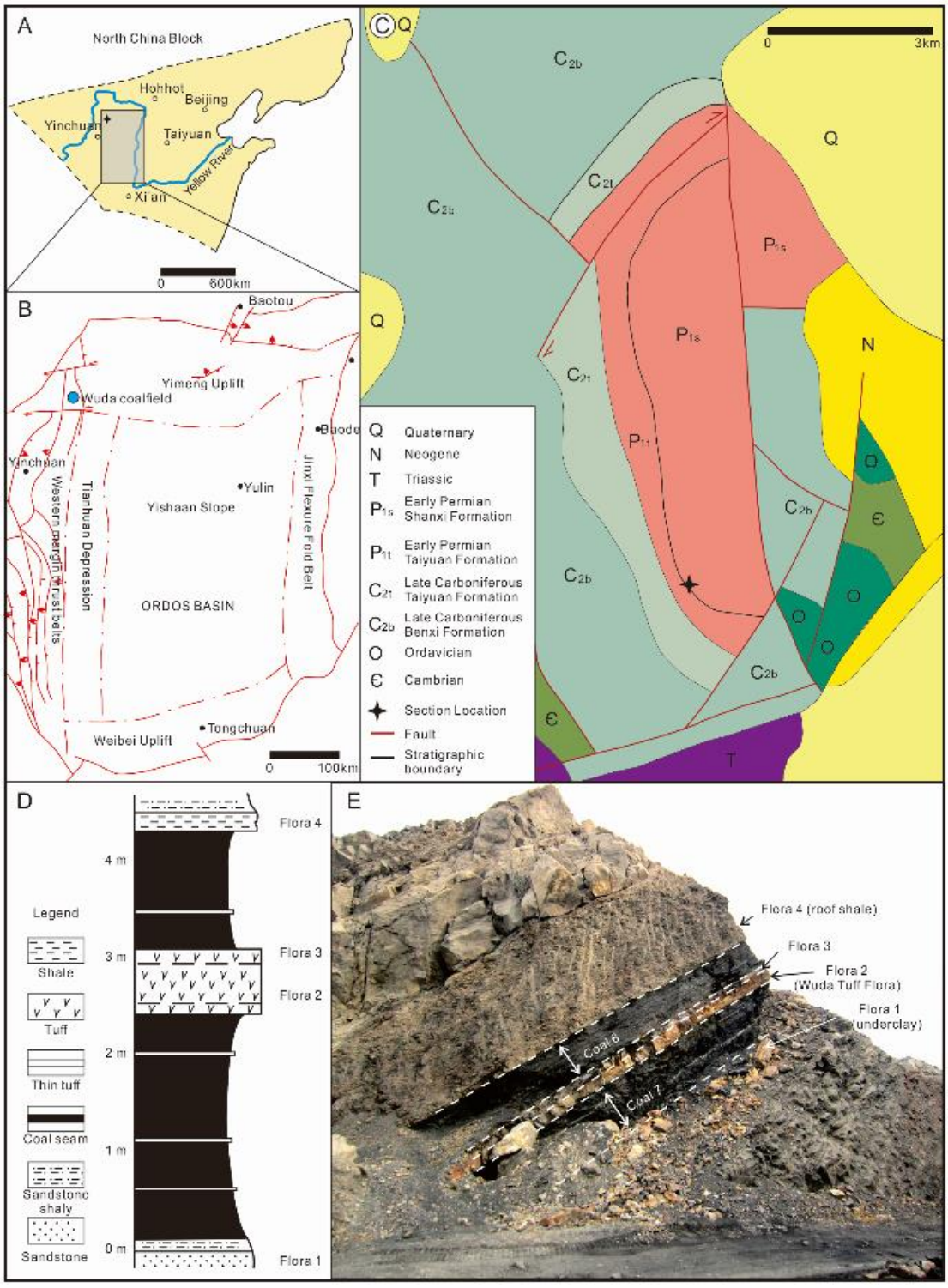
A
North China Block
Hohhot
Beijing
Yinchuan
Taiyuan
Yellow River
Xi'an
0
600km
B
Baotou
Yimeng Uplift
Wuda coalfield
Baode
Yinchuan
Yulin
Western margin thrust belts
Tianhuan Depression
Yishaan Slope
Jinxi Flexure Fold Belt
ORDOS BASIN
Tongchuan
Weibei Uplift
0
100km
Q Quaternary
N Neogene
T Triassic
P1s Early Permian Shanxi Formation
P1t Early Permian Taiyuan Formation
C2t Late Carboniferous Taiyuan Formation
C2b Late Carboniferous Benxi Formation
O Ordavician
Є Cambrian
Section Location
Fault
Stratigraphic boundary
C
0
3km
D
Flora 4
4 m
Legend
Shale
3 m
Flora 3
Flora 2
Tuff
Thin tuff
2 m
Coal seam
1 m
Sandstone shaly
Sandstone
0 m
Flora 1
E
Flora 4 (roof shale)
Flora 3
Flora 2
(Wuda Tuff Flora)
Flora 1
(underclay)
Coal 6
Coal 7

Figure 1

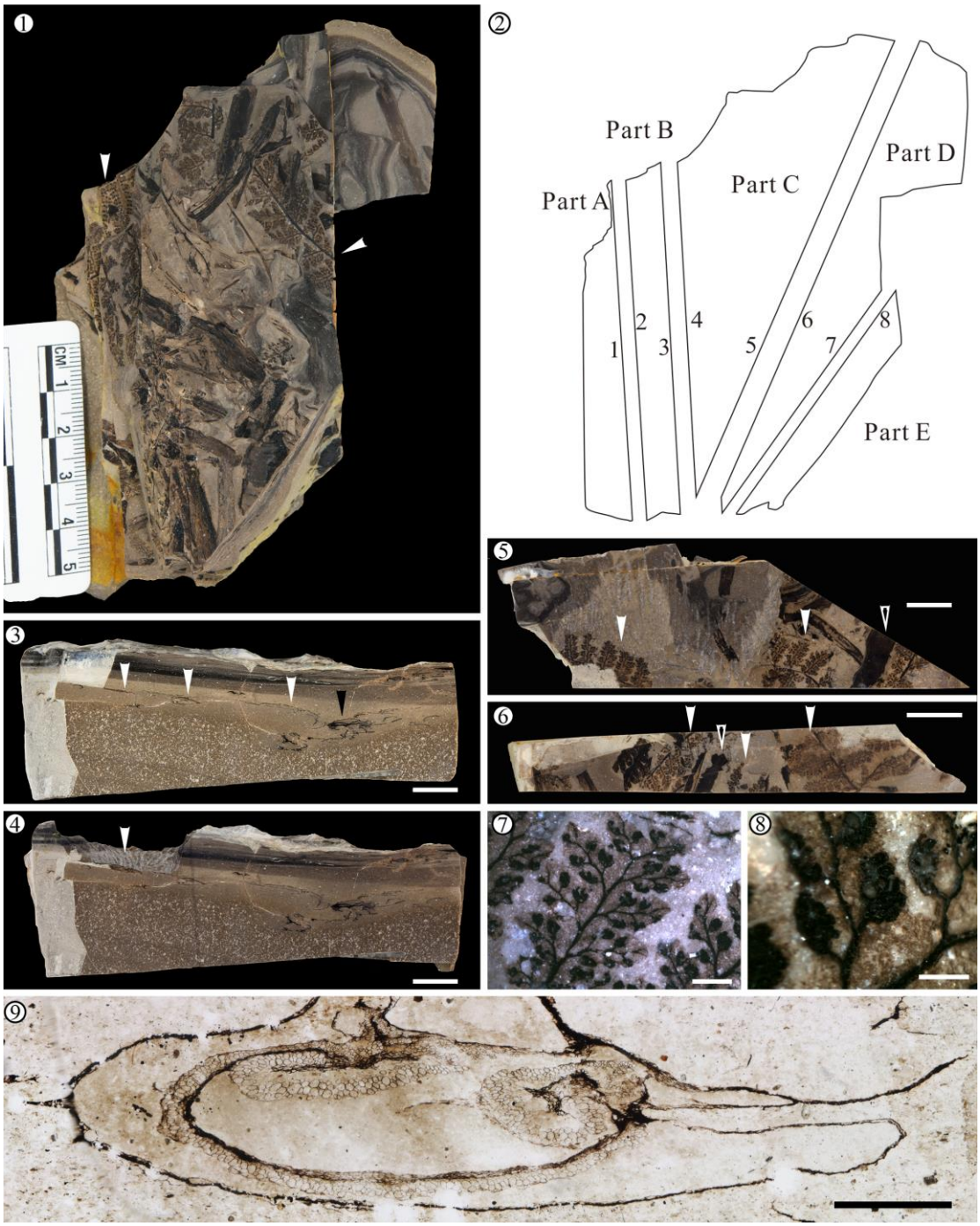

777

778 Plate I

779

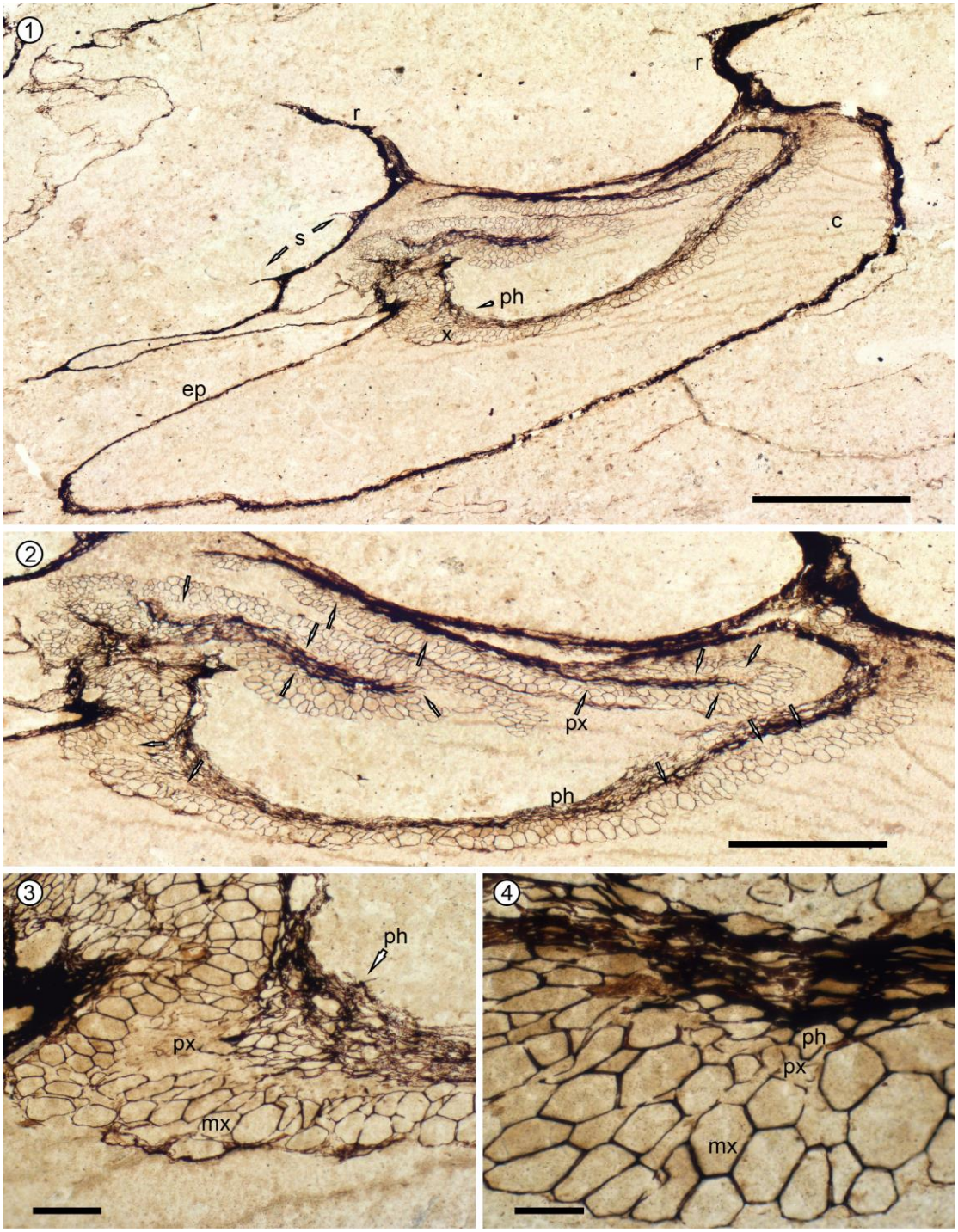

780

781 Plate II

782

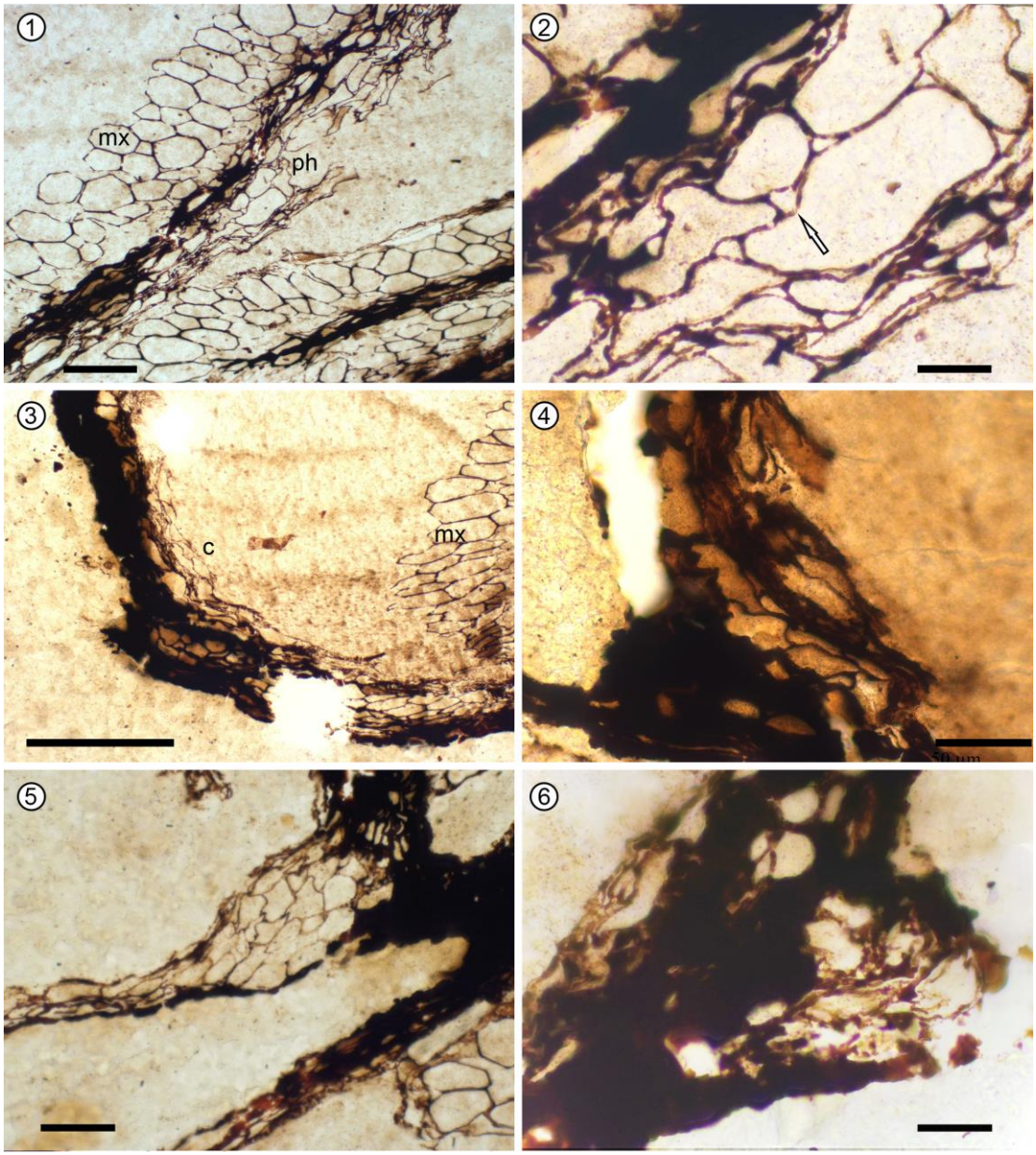

Plate III

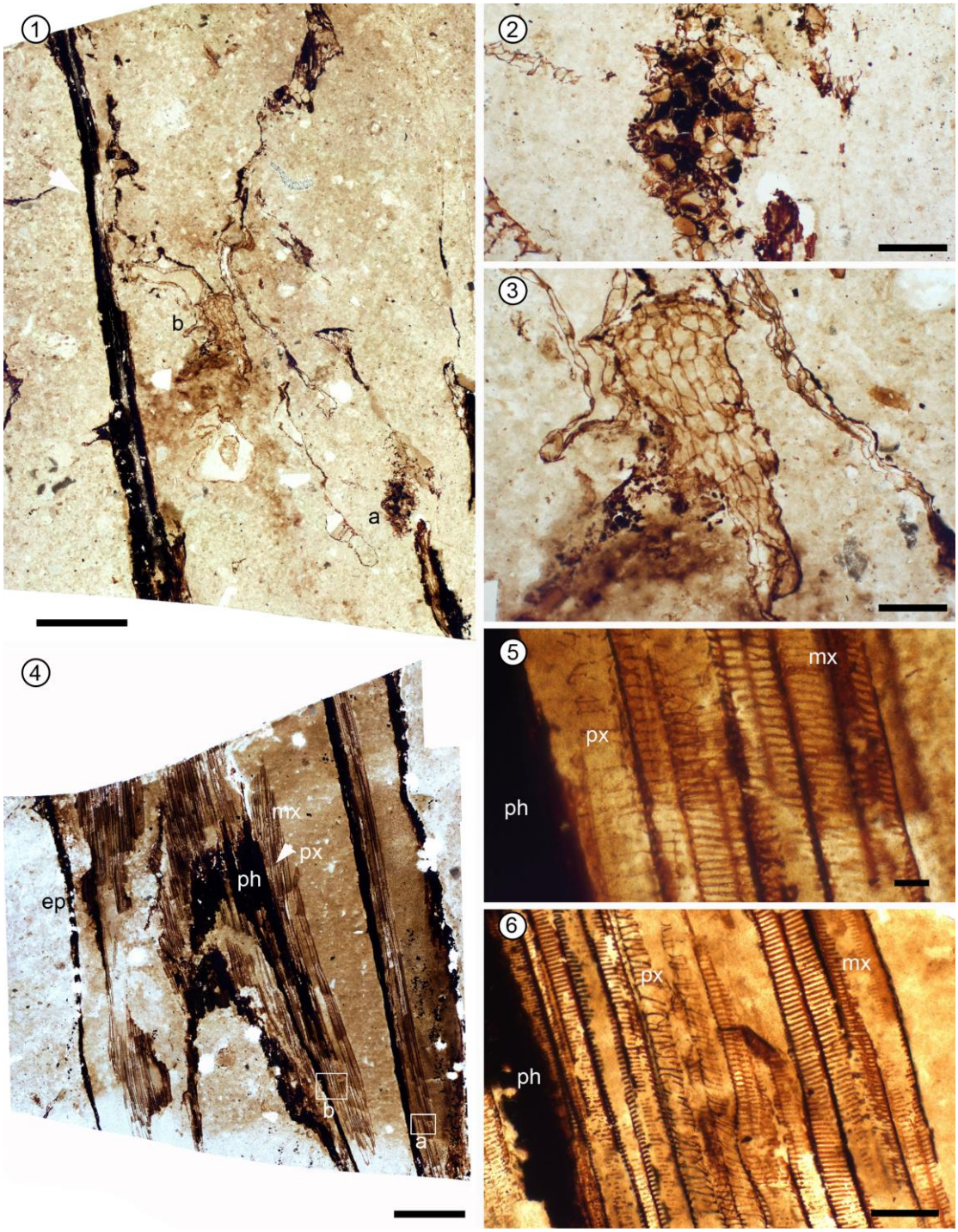

786

787 Plate IV

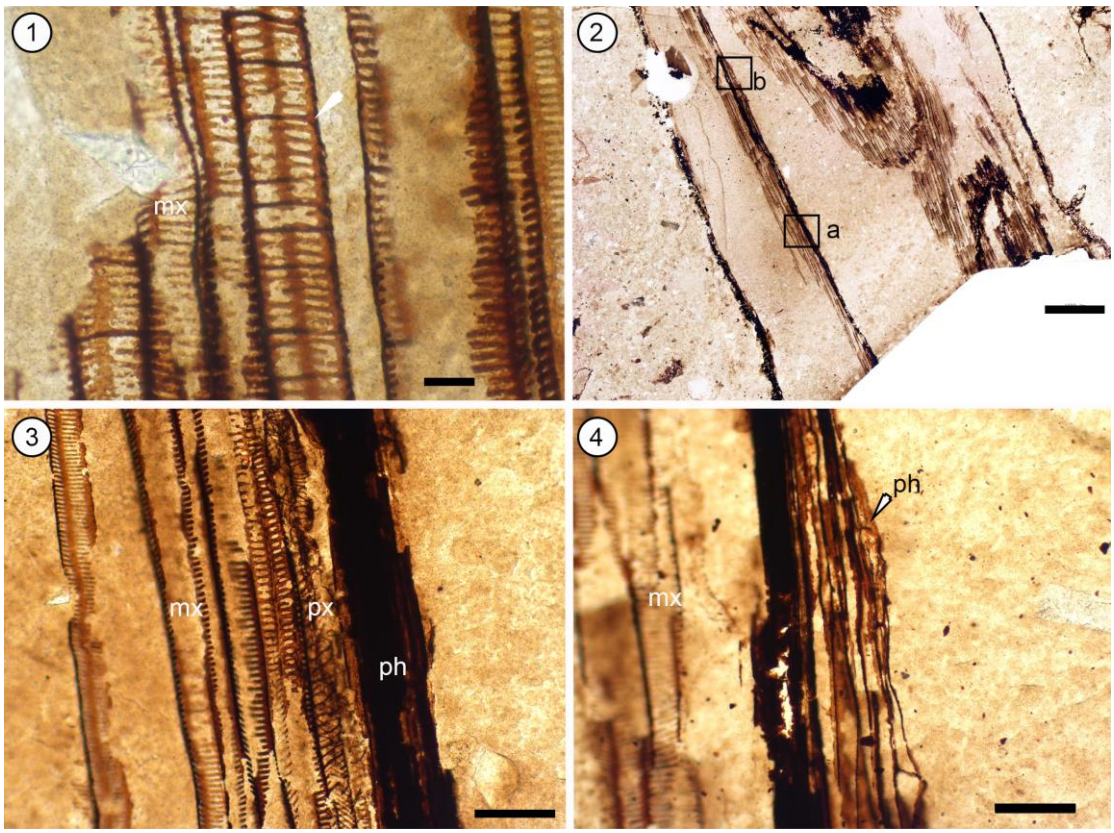

Plate V